

Climate has contrasting direct and indirect effects on armed conflicts

David Helman^{1,2,*}, Benjamin F. Zaitchik¹ and Chris Funk^{3,4}

¹ Department of Earth and Planetary Sciences, Johns Hopkins University, Baltimore, Maryland, USA

² Currently at the Department of Soil & Water Sciences, The Robert H. Smith Faculty of Agriculture, Food & Environment, Rehovot, and Advanced School for Environmental Studies, The Hebrew University of Jerusalem, Jerusalem, Israel

³ Earth Resources Observation and Science Center, U.S. Geological Survey, Sioux Falls, South Dakota, USA

⁴ Climate Hazards Center, University of California, Santa Barbara, Santa Barbara, California, USA

There is an active debate regarding the influence that climate has on the risk of armed conflict, which stems from challenges in assembling unbiased datasets, competing hypotheses on the mechanisms of climate influence, and the difficulty of disentangling direct and indirect climate effects. We use gridded historical non-state conflict records, satellite data, and land surface models in a structural equation modeling approach to uncover the direct and indirect effects of climate on violent conflicts in Africa and the Middle East (ME). We show that climate–conflict linkages in these regions are more complex than previously suggested, with multiple mechanisms at work. Warm temperatures and low rainfall direct effects on conflict risk were stronger than indirect effects through food and water supplies. Warming increases the risk of violence in Africa but unexpectedly decreases this risk in the ME. Furthermore, at the country level, warming decreases the risk of violence in most West African countries. Overall, we find a non-linear response of conflict to warming across countries that depends on the local temperature conditions. We further show that magnitude and sign of the effects largely depend on the scale of analysis and geographical context. These results imply that extreme caution should be exerted when attempting to explain or project local climate–conflict relationships based on a single, generalized theory.

1. Introduction

Although there is a suggested linkage between violent conflict and climate, the underlying mechanisms of the link are still under debate^{1,2}. One commonly suggested mechanism is of climate–conflict link through economic disruption^{3,4}. Though plausible, there is currently no robust evidence for such a direct climate–economy–conflict nexus⁵. Instead, many studies suggest that climate-driven depressions may lead to conflict through a combination of socioeconomic and political failure, particularly in agricultural dependent regions where people depend directly on such resources⁴. That is, climate influences economy, which influences social and political systems relevant to conflict.

It is also possible that the climate–conflict connection is less direct, operating through the influence that climate-induced changes in economy, food security, or group interactions cascade to influence the probability of inter-group violent conflicts. This indirect influence is relevant to theories like the “engagement” hypothesis, which claims that when climate crisis

45 reduces economic productivity people become more likely to engage in conflicts than in
46 economic activities^{6,7}, or the “inequality” hypothesis, which argues that conflict may upsurge
47 when climate crisis increases economic inequality because of increasing efforts to redistribute
48 assets⁸, and the “state weakness” hypothesis that suggests a weakening of governmental
49 institutions and their ability to suppress violence due to decline in economic productivity
50 following climate crisis⁹. All these, suggest that climate has an indirect rather than a direct
51 effect on violent conflicts¹⁰.

52 While these hypotheses were first studied in the context of civil wars and other state-
53 engaged conflicts, research in the past decade on communal, non-state violence has also
54 emphasized the mediated pathways through which climate can influence conflict. This
55 includes the potential for harmful climate anomalies like drought to drive conflicts in times of
56 scarcity due to resource competition, lowered opportunity cost, or other mechanisms^{11,12}. But
57 it also includes the potential for beneficial climate anomalies to increase conflict due to rent
58 seeking or available resources to support violent activities during times of abundance^{13,14}.
59 Studies have also found that climate variability in either direction can lead to increased
60 conflict, due to the presence of multiple mechanisms driving conflict or to the presence of
61 qualitatively different categories of conflict^{15,16}.

62 The direct influence of climate on individual tendency toward violence may also play a
63 role. Warming, for example, has been shown to enhance violence through a direct
64 psychological mechanism [the General Aggression Model – GAM] by making people
65 uncomfortable and irritated¹⁷. Alternatively, warming may enhance violence in cooler
66 environments because warm, more favorable weather conditions lead to increased activity
67 and interaction between people [Routine Activity Theory - RAT], which may lead to more
68 opportunities for conflict¹⁸.

69 To assess climate impacts on violence and uncover whether the underlying mechanisms
70 are direct, indirect, or a combination of both, ‘non-climatic’ effects must be isolated. Some
71 studies do this by pooling data across locations and applying statistical models that control
72 for non-climatic factors explicitly. The climate influence is then examined through its partial
73 effect on violence^{19,20}. Other researchers argue that controlling for non-climatic factors
74 explicitly can absorb most of the climatic impact and, therefore, may result in an
75 underestimation of the climate effect²¹. For this reason, it is argued, pooling analysis across
76 sites is misleading, and climate effects should be studied by comparing each place with itself
77 in time rather than with other places. Studies using this site self-comparison approach have
78 reached more conclusive results regarding climate impacts on violence than cross-sectional
79 studies using explicit controls^{21,22}. The problem with this self-comparison approach,
80 however, is that it cannot identify underlying ‘universal’ mechanisms because the analysis is
81 conducted location-by-location rather than across locations²³.

82 To some extent, the contrasting results published in the literature is a reflection of that
83 disagreement²⁴, with this inconsistency leading to criticism of climate-conflict research.
84 Some researchers have claimed that the link between climate and conflict is unsupported by
85 the evidence²⁵. Furthermore, researchers have been accused of bias in their approach to the
86 problem^{26,27}. Yet, most experts do believe that climate has a significant effect on human
87 conflicts²⁸, though the generality of the links and the underlying mechanisms are yet to be
88 established.

89 Here we use a powerful assemblage of disaggregated data (table S1), which includes the
90 Uppsala Conflict Data Program (UCDP) conflict dataset²⁹ as well as climatic [temperature
91 and rainfall anomalies] and non-climatic [anomalies in water availability, Infant Mortality
92 Rates, agricultural yield, and economic welfare] datasets derived from satellites and land

93 surface models to test generalizability of climate-conflict relationships from national to
94 continental scale. To leverage the strengths of the two approaches – the site self-comparison
95 and the use of explicit controls in a cross-sectional analysis – and explore general
96 mechanisms, we make use of structural equation modeling [SEM] ³⁰ in which non-climatic
97 factors are explicitly controlled while direct and indirect effects of climate – through the non-
98 climatic factors – are quantified in order to uncover the underlying mechanisms.

99 We choose to focus on non-state conflicts rather than civil wars because small-scale
100 conflicts are likely to be more sensitive to environmental and climatic changes^{19,28}. Also, we
101 focus on Africa and the Middle East [ME] because these two regions experienced a large
102 number of armed conflicts in the last three decades (Fig. 1A). Finally, we hypothesize that
103 comparing these two ethnically and culturally distinct, but yet geographically close regions
104 may reveal contrasting mechanisms.

105 **2. Data and Methods**

106 Armed Conflict Dataset

107 *The UCDP Geolocated Violent Conflict Dataset*

108 We used the most updated Georeferenced Event Dataset [GED] Global version 18.1
109 (2017) of the Uppsala Conflict Data Program [UCDP ²⁹] for location-specific information on
110 armed conflicts in Africa and the ME. The GED.v18.1 is UCDP’s most disaggregated data
111 set, covering individual events of organized violence as phenomena of lethal violence
112 occurring at a given time and place. Events are sufficiently fine-grained to be geo-coded
113 down to the level of individual villages, with temporal durations disaggregated to single,
114 individual days ³¹. Conflicts used here are “non-state” conflicts, defined by UCDP as “the use
115 of armed force between two organized armed groups, neither of which is the government of a
116 state, which results in at least 25 battle-related deaths in a year” ³¹. Information on specific
117 conflict is freely available at [www.ucdp.uu.se], and questions regarding the definitions used
118 by UCDP as well as the content of the dataset can be directed to that site. In the GED dataset,
119 each conflict has a unique identifier [conflict ID], while the start date is recorded as precisely
120 as possible with the level of precision for day, month and year indicated alongside
121 [“Startprec” variable in GED.v18.1].

122 For our analysis we used conflicts indicated with a “Startprec” level of at least 5 meaning
123 that “Day and month are assigned, year is precisely coded; day and month are set as precisely
124 as possible”. A violent event was defined as a coded event, which is unique in terms of
125 starting and ends dates, and is not a continuation or part of a previous event. All events were
126 first binned at a spatial resolution of 0.5° x 0.5° for African and ME regions by summing the
127 total number of events per grid per year. Events were assigned to a specific year by indicated
128 starting date. A layer of violent events by 0.5° per year was produced alongside another layer
129 with the sum of events for the entire period of 1990 – 2017 (Fig. 1A). Because we look for
130 effects on the risk of violent conflict outbreak, each layer was converted into a binary layer in
131 which each grid was assign a value of 1 for grids that experienced violence during this year,
132 or 0 for grids that did not experience violence. Although we had information on violence for
133 1990- 2017, we used only layers for years 1992 – 2012 in the SEM analysis because this was
134 the period in which we had a complete data set of climate and non-climate variables (see
135 below). We included Syria in our analysis, but excluded the years after 2010 because of the
136 poor information on violent events during the period of the Syrian civil war ^{31,32}.

137 Climate Data

138 We used temperature and rainfall data sets, described below, to seek for direct and indirect
139 effects of temperature and rainfall anomalies on non-state conflicts. Direct effects of climate
140 could be only at the time of occurrence, so relationships were analyzed for the same year
141 (present-year violence). However, indirect effects – through food, water, and economic
142 welfare – may occur at a certain time-lag. Because linking climate anomalies indirectly to
143 conflicts at too long time-lag periods may be problematic (because of the uncertainty that
144 such climatic changes are really related to conflicts many years after), we looked only for
145 links with a one-year time lag (next-year violence).

146 *Temperature anomaly*

147 We used monthly maximum temperatures from the newly derived Climate Hazards
148 center Infrared Temperature with Stations [CHIRTS] dataset³³. CHIRTS provides monthly
149 2-m maximum air temperatures at a high spatial resolution of 0.05° and a quasi-global
150 coverage [60°S-70°N] from 1983 to 2016. Temperature estimates are derived using a
151 combination of thermal imagery from a constellation of geostationary satellites, a high-
152 resolution climatology from the Climate Hazards Center’s Tmax climatology, and in situ
153 monthly 2-m Tmax air temperature observations obtained from the Berkeley Earth and
154 Global Telecommunication System [GTS]. We used the temperature estimates from CHIRTS
155 because these were shown to be suitable for monitoring temperature anomalies and extremes
156 in data-sparse regions like Africa and the ME³³. The high spatial resolution temperature
157 estimates were averaged over 0.5° x 0.5° for the period of the analysis [1992-2012], and the
158 yearly anomaly was calculated per grid as z-score [the long-term mean annual temperature
159 was subtracted from the specific year mean temperature and divided by the standard
160 deviation].

161 *Rainfall anomaly*

162 For rainfall anomaly, we used the Climate Hazards group Infrared Precipitation with
163 Stations [CHIRPS] dataset, available at a high spatial resolution of 0.05°³⁴. This product is
164 quasi-global precipitation product with daily to seasonal time scales and a 1981 to near real-
165 time period of record. CHIRPS uses three main types of information: (1) global 0.05° rainfall
166 climatologies, (2) time-varying grids of satellite-based rainfall estimates, and (3) in situ
167 rainfall observations. CHIRPS is built on ‘smart’ interpolation techniques and high
168 resolution, long period of record estimates based on infrared Cold Cloud Duration [CCD]
169 observations as well as on satellite information, used to represent ungauged locations.
170 CHIRPS is very reliable in regions like Africa and the ME where most rainfall products fail
171 to accurately represent the high temporal and spatial variability in rainfall³⁵ due to the sparse
172 gauge network in this region³⁶.

173 We used CHIRPS monthly rainfall sums [from January to December] to assess the
174 annual rainfall anomaly for 1992 – 2012, calculated as z-scores [the long-term mean annual
175 rainfall subtracted from specific year rainfall sum, divided by the standard deviation]. Each
176 year a z-score map was produced while pixels were aggregated to the spatial resolution of the
177 analysis [0.5° x 0.5°]. Annual rainfall is not a comprehensive proxy for conflict-relevant
178 rainfall variability, but it offers a practical, objective measure that can be applied consistently
179 across our diverse study domain.

180 Non-Climate Data

181 *Infant Mortality Rate*

182 As a proxy of socioeconomic development, we used information on infant mortality rate
183 [IMR] from the Global Subnational Infant Mortality Rates, Version 1 [GSIMR.v1]³⁷. The

184 GSIMR.v1 dataset is produced by the Columbia University Center for International Earth
185 Science Information Network [CIESIN] at a high spatial resolution of 5 km and is freely
186 available for download as a raster data layer from [<http://www.ciesin.columbia.edu/povmap>].
187 The GSIMR.v1 consists of IMR estimates for the year 2000, which was collected from vital
188 registration data, surveys and models or estimated using reported live births and infant deaths
189 data. Though our analysis spans the period of 1992 – 2012, we assume that the 2000
190 GSIMR.v1 is, in average, representative of the entire period following previous studies³⁸.
191 The IMR is calculated as the number of deaths of infants of less than one year old divided by
192 the number of live births and multiplied by 1000. We preferred using the IMR as a proxy of
193 poverty and socioeconomic status instead of using other variables because measures like
194 Gross Domestic Product [GDP] or population living on less than one U.S. dollar per day, are
195 difficult to obtain at sub-national levels, particularly for the regions of this study. Moreover,
196 using IMR has several advantages over other socioeconomic metrics. For example, IMR is a
197 highly standardized measure compared to other measures, which means that it can be used to
198 compare between countries with different economic systems better than GDP, for example³⁸.
199 Also, IMR is less likely to be influenced by skewed wealth distribution. And, information on
200 IMR is available for ~90% or more of the population in medium and low-income countries.
201 The original 5-km IMR data layer was binned at the spatial resolution of 0.5° x 0.5°, which is
202 the resolution of the analysis and used as a static map layer.

203 *Distance to Border*

204 Distance from/to political borders was assessed using a geographical information system
205 and a shapefile layer of the political borders of African and the ME countries. The minimal
206 distance from each grid cell to the nearest border was recorded and used in the SEM analysis.
207 Because this information is static [i.e., it does not change during the period of analysis] the
208 same value was used in all years.

209 *Agricultural Dependence*

210 To assess agricultural dependence as share of cropland area in a 0.5° grid cell, we used
211 the Climate Change Initiative [CCI] of the European Space Agency [ESA] Land Cover
212 product. The ESA CCI product is an annual global land cover time series from 1992 to 2015
213 [now available also for 2016 to 2018], available at an unprecedented high spatial resolution of
214 300 m (<https://www.esa-landcover-cci.org/?q=node/175>). This unique dataset was produced
215 by reprocessing and interpretation of daily surface reflectance of five different satellite
216 missions. It uses the full archive of MERIS [2003–2012], with 15 spectral bands and 300 m
217 spatial resolution and the 1 km time series from AVHRR [1992–1999], SPOT-VGT [1999–
218 2013] and PROBA-V [2014 and 2015]. The baseline was established through MERIS data
219 and use of machine learning and unsupervised algorithms³⁹.

220 The advantage of this product over other products that are derived from several
221 observation systems is that it maintains a good consistency over time. This is done by
222 confirming changes observed in earlier and later MERIS era satellites via back- and forward
223 checking through the 10-year MERIS base-line LC maps. The ESA CCI LC product was
224 evaluated with a global independent validation dataset according to international standards,
225 testing the accuracy of both LC classes and LC change in time³⁹. It was also found accurate
226 through a comparison using country-level information provided by the Food and Agriculture
227 Organization of the United Nations [FAO-STAT] in several countries⁴⁰.

228 We used the 1992 – 2012 ESA CCI LC maps to classify pixels into agricultural *versus*
229 non-agricultural classes. More specifically, LC classes #10, 20, 30, and 40, which include
230 also mosaics of croplands and natural vegetation, were designated as agricultural pixels while

231 others were assigned as non-agricultural pixels. We then aggregated the 300-m pixels into the
232 coarser resolution of 0.5° [resolution of analysis] and calculated the total share of agricultural
233 area in each 0.5° grid cell [as the percentage of total area]. These estimates were used to
234 examine influence of agricultural dependence [larger crop share of area equals higher
235 agricultural dependency³⁸] on violence risk as well as to derive yearly change in agricultural
236 yield production [see next sub-section].

237 *Yield Production*

238 To quantify changes in agricultural yield production, we used NASA's VIPPHEN EVI2
239 satellite product⁴¹. The VIPPHEN EVI2 data product is provided globally at 0.05° [~5600
240 meters] spatial resolution and contains 26 Science Datasets [SDS], including phenological
241 metrics such as the start, peak, and end of season as well as the maximum, average, and
242 background calculated EVI2 (https://lpdaac.usgs.gov/products/vipphen_evi2v004/). It is
243 currently the longest and most consistent satellite-based global vegetation phenology product
244 available. VIPPHEN SDS are based on the daily VIP product series and are calculated using
245 a 3-year moving window average to eliminate noise.

246 The modified 2-band enhanced vegetation index [EVI2] is highly correlated with the
247 commonly-used EVI⁴², which was found to be useful for tracking changes related to
248 vegetation dynamics⁴³ as well as gross primary productivity⁴⁴. EVI2 differs from the
249 traditional EVI by its use of two bands, the red and near infrared, instead of the use of three
250 bands, which includes also the blue band in the index calculation. The integral over the
251 growing season of EVI2 [EVI_{GSI}; fig. S1] was used here as a proxy of agricultural yield
252 production. Growing season integrals of vegetation indices are usually well correlated with
253 biomass of green tissues, particularly in annual vegetation systems⁴⁵⁻⁴⁷, and as such may
254 serve as a good proxy of crop yield production⁴⁸. EVI_{GSI} was derived per year for
255 agricultural pixels with > 50% of agricultural area cover [estimated from the ESA CCI LC
256 300 m product]. Pixels with < 50% of agricultural area cover were discarded from the
257 analysis in order to remove influences of non-agricultural vegetation systems on EVI_{GSI}.

258 Because agricultural fields differ in crop type and different crop types may have similar
259 EVI_{GSI} values, we used the relative anomaly of EVI_{GSI} as a proxy of relative anomaly in local
260 yield production instead of the absolute EVI_{GSI} value. In order to assess the validity of this
261 approach, we compared yearly anomalies of national yield production, derived from the food
262 and agriculture data provided by the Food and Agriculture Organization of the United
263 Nations [FAO-STAT⁴⁹], with country-level EVI_{GSI} anomalies (z-scores) for the period of
264 analysis [1990-2012; see *Supplementary Material* and figs. S2 to S5]. Yield is provided in
265 FAO-STAT as hectograms per hectare [hg/ha] for cereals, citrus fruit, coarse grain, fibre
266 crops, oil-crops, pulses, roots and tubers, treenuts, vegetables and fruits
267 (<http://www.fao.org/faostat/en/#data/QC>). The total annual yield and the long-term mean
268 annual yield [1990-2012] from FAO-STAT were calculated to derive the relative anomaly in
269 percentages of the long-term average yield [%]. The same procedure was applied for the
270 calculation of the EVI_{GSI} annual anomaly [as percentages of the mean EVI_{GSI}].

271 *Satellite Night-time Lights as A Proxy of Economic Welfare*

272 We used night-time lights intensity from the Defense Meteorological Satellite Program
273 [DMSP⁵⁰] to estimate grid-based economic welfare status and dynamics in Africa and the
274 ME. This night-time light product dates back to 1992 and is considered to be well correlated
275 with GDP, built-up area, energy consumption, poverty, and other socioeconomic welfare
276 variables⁵¹⁻⁵⁴. We used the DMSP yearly average stable night-time lights intensity product at
277 a spatial resolution of 30 arcsec [~1km] for 1992-2012 to calculate the percentage area of

278 light per pixel [LitArea]. Method was followed by the described in ⁵⁵. In short, light intensity
279 in DSMP is given as a digital number [DN] from 0 to 100 for each pixel. A DN threshold
280 value is then used to assign each pixel with a binary 1/0 for presence/absence of light. The
281 threshold of DN>31 was used following ⁵⁵. The total LitArea per 0.5° grid – i.e. the sum of
282 the squared kilometers of light in a 0.5° grid cell – was derived by aggregating pixels with
283 values to the spatial resolution of the analysis. The total number of square kilometers was
284 then converted into square meters and divided by the population density in the same grid cell
285 to derive the relative LitArea [R-LitArea].

286 This was done because places with denser populations are expected to have higher
287 LitArea, which will not necessarily indicate a higher economic welfare status but may just
288 reflect a larger build-up area. By dividing the LitArea by the population density, we thus
289 normalize for such an effect, remaining with a relative measure of economic welfare. We
290 used the WorldPop dataset [www.worldpop.org.uk] for grid-based information on population
291 density. This dataset uses an ensemble learning method for classification, combining 30-m
292 Landsat Enhanced Thematic Mapper (ETM) satellite imagery for high-resolution mapping of
293 settlements and gazetteer population numbers to produce gridded population density maps at
294 high spatial resolutions ⁵⁶. Yearly population maps for Africa and the ME are available from
295 2000 to date [downloaded from: <https://www.worldpop.org/project/categories?id=3>] at the
296 same resolution of the DSMP dataset [1km x 1km]. We used simple linear interpolation to
297 derive population density for 1992-1999, and aggregated the original resolution to the coarse
298 spatial resolution of the analysis [0.5° x 0.5°]. R-LitArea was derived per 0.5° grid cell as the
299 ratio between LitArea and population density. Finally, R-LitArea z-score was calculated to
300 get yearly economic welfare anomaly.

301 *Grid-Based Water Resources Information from Land Surface Models*

302 Gridded estimates of soil moisture and hydrological fluxes, along with river network
303 estimates of streamflow, were generated using the NASA Land Information System [LIS] ⁵⁷
304 software frameworks. In this implementation, LIS was implemented using the Noah-
305 MultiParameterization [Noah-MP] ⁵⁸ Land Surface Model and the Hydrological Modeling
306 and Analysis Platform [HyMAP] ⁵⁹ river routers. All simulations were performed using
307 meteorological forcing data drawn from the NASA Modern Era Reanalysis for Research and
308 Applications, v2 [MERRA-2] ⁶⁰, with the exception of precipitation, which came from the
309 Climate Hazards InfraRed Precipitation with Stations, v2 [CHIRPSv2] ³⁴ dataset. Simulations
310 were performed at 0.1° horizontal resolution with a timestep of 30 minutes. A 30-year spin-
311 up was performed to equilibrate model soil moisture states, and the simulation was then run
312 from 1990-2018. In this application, Noah-MP was used with four soil moisture layers
313 [thicknesses of 0.1, 0.3, 0.6 and 1.0 m, descending from the surface] and a simple unconfined
314 aquifer. Soil moisture and surface runoff were aggregated to the spatial resolution of the
315 analysis and the z-score of each 0.5° grid cell was calculated to derive the inter-annual
316 anomaly.

317 **4. Assessing Direct and Indirect Causal Effects**

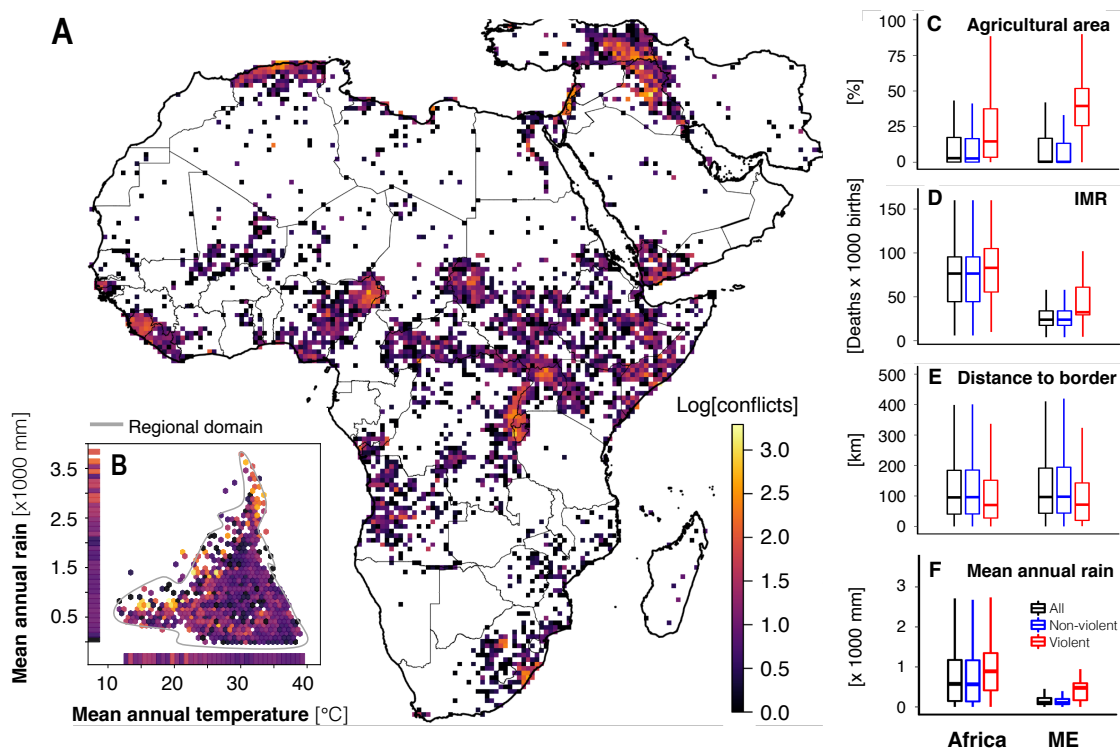
318 The SEM approach was used because it allows to evaluate direct and indirect effects of
319 climate and non-climate factors on violence risk, as well as to quantify relationships among
320 factors. In that sense, SEM has an advantage over univariate regression approaches, such as
321 general additive models (GAM) and general linear models (GLM), because it can be used to
322 evaluate direct effects while controlling for joint effects. For example, it provides a way to
323 evaluate the direct effect of yield on conflict risk while controlling for the joint effects of
324 climate variables on yield and conflict. The ability of SEM to quantify direct and indirect

325 relationships makes it particularly suited for confirming causal relationships based on *a priori*
 326 hypotheses.

327 Our SEM was developed based on a conceptual model designed to test *a priori*
 328 hypothesis that relates climate to food and water security, economic welfare and – directly
 329 and indirectly – to conflict risk ⁶⁻⁹. It was then applied on a 0.5° grid basis in a time-for-space
 330 model design for 1992-2012 (see *Supplementary Material*). The SEM model was applied for
 331 Africa, the ME, and both regions together, as well as for each country separately. To enable
 332 comparison between datasets with different normal distributions, we used the relative
 333 anomaly – quantified as a standard score [z-score] – instead of the absolute values of the
 334 climate and non-climate factors. The control variables [IMR, agricultural dependence and
 335 distance to border], on the other hand, were maintained with their absolute values in order to
 336 quantify the absolute influence of these factors on the climate-conflict relationships. The
 337 conflict data was converted to a binary dataset, with 0 for non-conflict and 1 for conflict
 338 years/grids. The results of the SEM are presented as standardized effects indicating the
 339 magnitude and sign of effect.

340 5. Results and Discussion

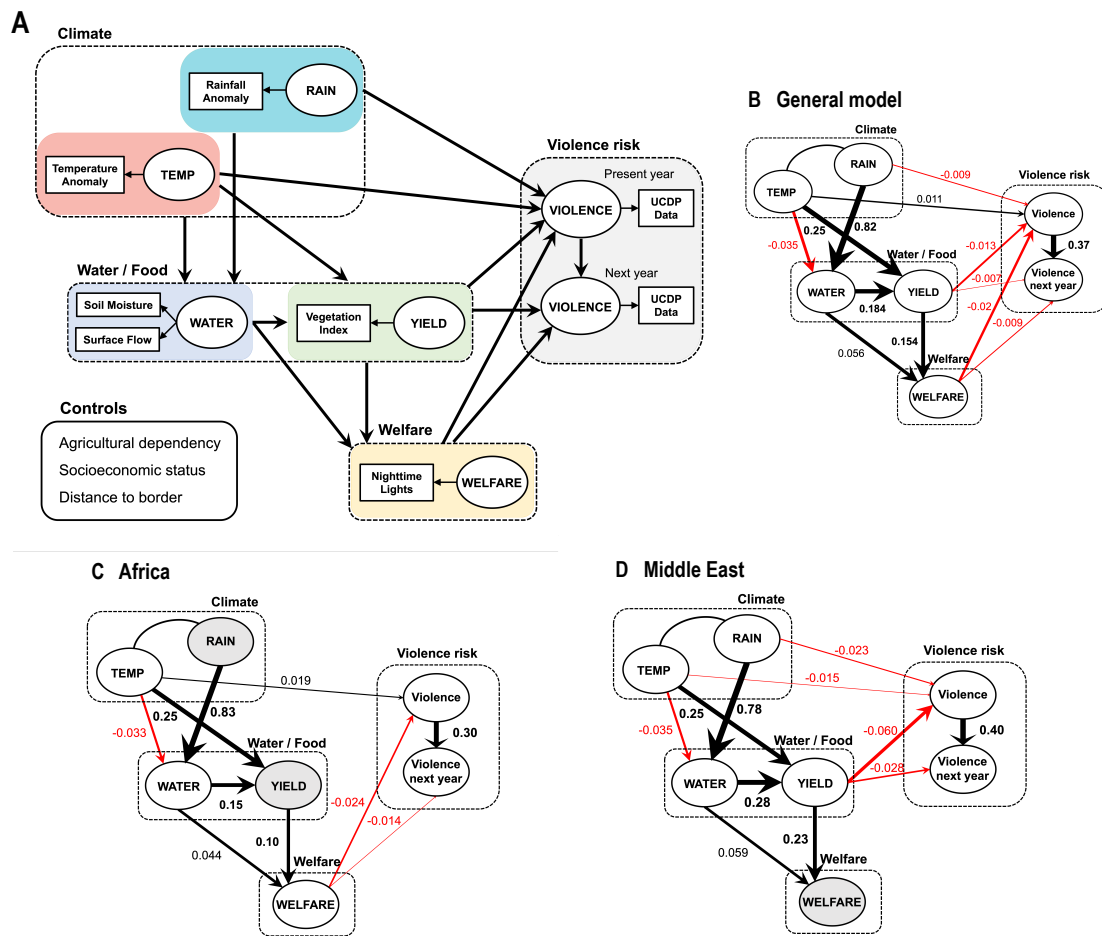
341 Non-state armed conflicts in the last three decades were not restricted to certain climatic
 342 conditions in Africa and the ME but rather occupied the entire climatic domain (Fig. 1B).
 343 Consistent with previous studies, violent conflicts are mostly found in agriculture dependent
 344 areas ³⁸, low socio-economic areas ⁶¹, and close to political borders ¹⁹ in both regions (Fig. 1C
 345 to E).



346 **Figure 1. Armed conflicts in Africa and the Middle East, and associated factors.** (A) Log number of armed
 347 conflicts by 0.5° grids for 1990 – 2017. (B) Mean annual rainfall and temperature binned by log number of
 348 conflicts. Gray line in (B) marks the region’s climatic domain (95th quantile of all grids). Boxplots show median,
 349 1st and 3rd quantiles of (C) relative agricultural area, (D) infant mortality rate (IMR), (E) distance to border, and
 350 (F) mean annual rainfall for violent (red), non-violent (blue) and all (violent + non-violent) grids. Violent grids
 351 are significantly different from non-violent grids in (C to F) at $P < 0.001$.

352 Non-state conflict grid cells also have higher than average rainfall (Fig. 1F) on account of the
 353 fact that population and agricultural activities are limited in arid regions. However, the
 354 association between violence and agricultural dependence was about four-fold stronger in the
 355 ME (Table 1), in spite of the larger average agricultural area in Africa [14% compared to 11%
 356 for the ME] (Fig. 1C), likely because of lower mean annual rainfall and therefore greater
 357 agricultural vulnerability to drought and water scarcity (Fig. 1F).

358 **Contrasting Climate Effects in Africa and the Middle East.** When applying the SEM to
 359 both regions together [general model] (Fig. 2B), yield and economic welfare had the strongest
 360 effect on present-year violence risk. Increases in yield and welfare reduced the chance of
 361 violence in both present and following year, while warming increased the risk and rain
 362 decreased this risk.



363
 364 **Figure 2. Structural equation models showing causal effects on conflict risk.** (A) The conceptual model.
 365 Models were applied to (B) Africa and Middle East together (general model), and to (C) Africa and (D) Middle
 366 East separately. Factors not affecting present-year violence are colored gray. Numbers alongside arrows indicate
 367 the standardized direct effects, with the color of the arrow indicating its sign (black for positive; red for negative)
 368 and width indicating its importance in the model. Constructs in our SEM are indicated by ovals while indicators
 369 are shown as rectangles. Only significant effects at $P < 0.05$ are shown.

370 While these results are in accordance to previously reported by others^{19,21,38}, unexpected
 371 complex climate-conflict links were revealed when SEMs were applied to each region
 372 separately (Fig. 2C and D). Warming increased the risk of violence in Africa (Fig. 2C) –
 373 similar to the general model – but unexpectedly decreased this risk in the ME (Fig. 2D).
 374 There was no effect of rain and yield on conflict risk in Africa and no effect of welfare in the
 375 ME. But there was a weak, though significant ($P < 0.05$), indirect negative effect of rain on

376 the risk of conflicts in Africa (Table 1), which was, surprisingly, through the effect of water
 377 availability on welfare and not through yield (Fig. 2C). This may be in part because satellite-
 378 based estimates of yield have limited skill in some conflict-prone African regions (fig. S3 and
 379 S4), but could also be due to a more complex link between rainfall, yield and violence than
 380 that drawn by our model. In all models, the risk of violence was greater in places where
 381 conflict already occurred in the previous year (Fig. 2B to D), which likely indicates the roles
 382 of political instability and historic background on such conflicts.

383 **Table 1.** Direct, indirect and total standardized effects of rain, temperature and yield anomalies on risk of violence,
 384 with and without explicit controls (marked in *italic*). High infant mortality rate (IMR) means low socio-economic
 385 status. Positive (negative) relationships are shown in black (red) font.

	Predictor	Without controls			With controls		
		Direct	Indirect	Total	Direct	Indirect	Total
General model	Rain	n.s.	-0.003**	-0.006**	-0.009**	-0.003**	-0.012**
	Temperature	0.011**	-0.003**	0.008**	0.011**	-0.004**	0.008**
	Yield	-0.009**	-0.003**	-0.013**	-0.013**	-0.003**	-0.016**
	<i>Agricultural area</i>	-	-	-	0.110**	-	-
	<i>IMR</i>	-	-	-	0.017**	-	-
	<i>Distance to border</i>	-	-	-	-0.033**	-	-
	Africa	Rain	n.s.	n.s.	n.s.	n.s.	-0.001*
Temperature		0.020***	n.s.	0.020***	0.019**	n.s.	0.019**
Yield		n.s.	-0.002***	n.s.	n.s.	-0.002**	n.s.
<i>Agricultural area</i>		-	-	-	0.073**	-	-
<i>IMR</i>		-	-	-	0.023**	-	-
<i>Distance to border</i>		-	-	-	-0.030**	-	-
ME		Rain	-0.015**	-0.009***	-0.025***	-0.023**	-0.012**
	Temperature	-0.026***	-0.011***	-0.037***	-0.015**	-0.014**	-0.028**
	Yield	-0.048***	n.s.	-0.047***	-0.060**	n.s.	-0.058**
	<i>Agricultural area</i>	-	-	-	0.264**	-	-
	<i>IMR</i>	-	-	-	0.083**	-	-
	<i>Distance to border</i>	-	-	-	n.s.	-	-

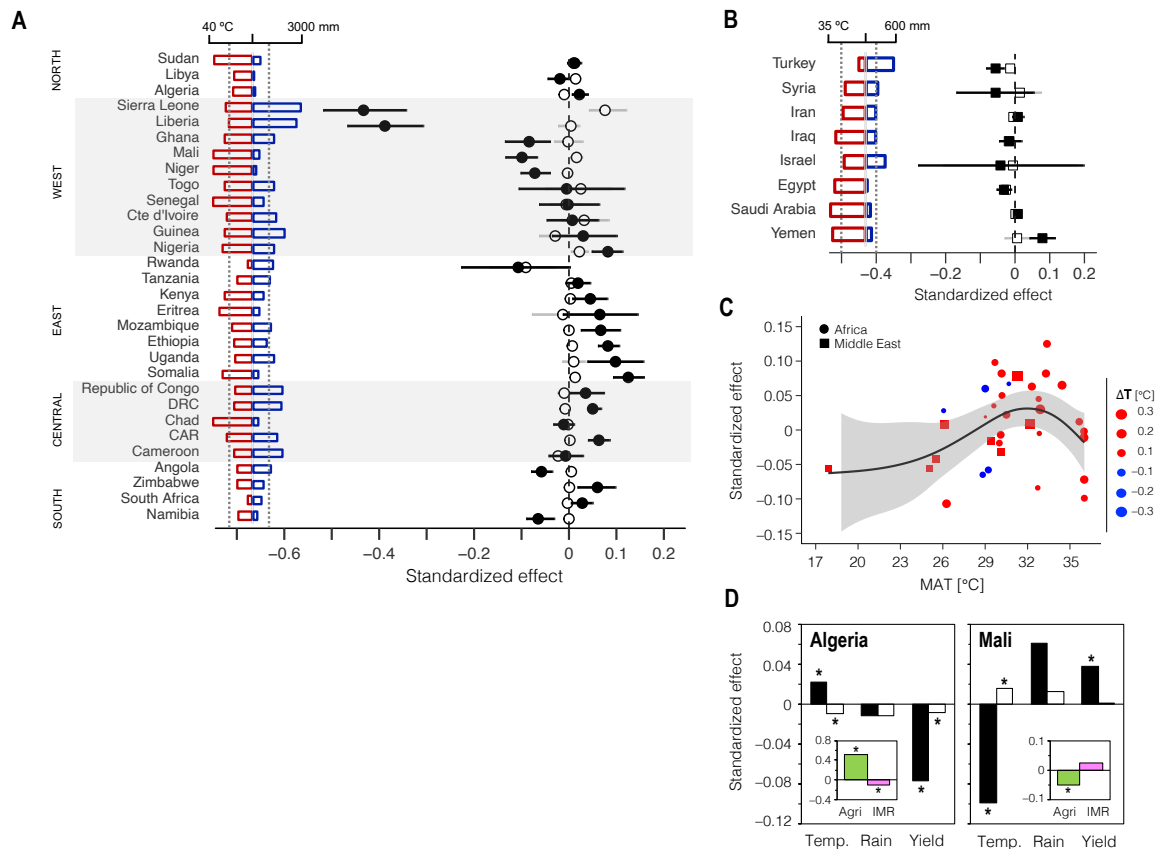
386 n.s. not significant; * $P < 0.05$; ** $P < 0.01$; *** $P < 0.001$

387 **A Non-Linear Response of Conflict to Warming.** To examine the generality of the
 388 contrasting effects, we further applied the SEMs per country. After analyzing the countries
 389 with enough conflicts to produce a statistically significant model (table S4), we found that not
 390 only ME countries, but also some African countries – particularly West African – had a
 391 negative, direct temperature effect on violence risk (Fig. 3A). This is although some of these
 392 countries are warmer than those showing a positive effect [e.g. East African countries], which
 393 would theoretically make them more vulnerable to heat-induced violence²³. In general, the
 394 country data show a non-linear relationship between the warming effect – i.e. the
 395 standardized direct effect of temperature anomaly on conflict risk – and the mean temperature
 396 conditions across countries, with a peak response at around 32°C (Fig. 3C). Countries with
 397 lower and higher mean annual temperatures (MAT) tend to exhibit lower effects of
 398 temperature anomalies on the risk of violence, with even negative effects in some cases.

399 An example of the latter is Sierra Leone and Liberia, which had the strongest effects,
 400 with a standardized negative effect of -0.43 and -0.39, respectively (Fig. 3A). These two
 401 countries are characterized by extremely warm and humid conditions, with high temperatures
 402 and large amounts of rainfall year-round (~3000 mm y⁻¹). Contrary to the GAM, which
 403 suggests that uncomfortable environmental conditions increase violent perceptions³, in this
 404 case uncomfortable extreme weather conditions [extra warming in already warm, humid
 405 countries] seemed to decrease the risk of violence.

406 Though under debate, previous studies suggest that physical aggression may have a
 407 rather complex, curvilinear response to heat^{62–64}. Aggression was shown to increase with

408 temperature rise, but decrease at excessive heat in several experimental settings, particularly
 409 when other negative-affect-producing factors are present ⁶⁴. The explanation given for this is
 410 that it is the urgent ‘need’ to escape or minimize discomfort which overcomes tendencies to
 411 aggressive behavior ⁶⁵. Taking this to Sierra Leone and Liberia, a further increase in
 412 temperature resulting in extremely unpleasant conditions might have increased discomfort
 413 and reduced the level of engaging in violence through such ‘escape’ mechanism. In this
 414 context, the RAT – suggesting that people interact more under pleasant conditions, which
 415 lead to more opportunities for violence – may be another possible explanatory mechanism ¹⁸.



416
 417 **Figure 3. Contrasting effects of temperatures on conflict risk.** Direct (close symbols) and indirect (open
 418 symbols) standardized effects of temperature on the risk of conflict from SEMs in (A) African and (B) Middle
 419 Eastern countries. Mean annual temperature and rainfall over 1992 – 2012 are shown. Effects with bars not
 420 crossing the vertical line in (A and B) are considered significant at $P < 0.05$. (C) The standardized direct effect of
 421 temperature vs. local temperature conditions expressed as the mean annual temperature [MAT]. Each symbol in
 422 (C) is a single country (Sierra Leone and Liberia are excluded for clarity), with the size indicating the average
 423 temperature change [ΔT] for the period of analysis and the line in depicting the nonparametric regression with
 424 corresponding confidence interval. (D) The standardized direct (black) and indirect (white) effects of temperature,
 425 rain, and yield on conflict risk in Algeria and Mali. Inserts in (D) show the effects of agricultural dependence and
 426 infant mortality rate (IMR) in Algeria and Mali. Asterisks denote significant effects at $P < 0.05$.

427 The positive and negative temperature effects in Yemen and Turkey (Fig. 3B) suggest
 428 that GAM is the primary mechanism in the ME rather than the RAT. The contrasting sign
 429 effect may be explained by a relaxation mechanism in which a decrease in unpleasant
 430 conditions – being warming in a cold area [Turkey] or cooling in a warm area [Yemen] –
 431 reduces the chance of violence ⁶⁶. This does not necessarily contradict the abovementioned
 432 ‘escape’ theory because warm and humid conditions in both Turkey and Yemen are more
 433 tolerable than in Sierra Leone and Liberia (Fig. 3A,B).

434 **Climate Effects in the Context of Geography and Ethnicity.** To further show how
435 complex this climate-conflict link may be, we focus on two cases –Algeria and Mali. Algeria
436 is the largest country in Africa, with an economy relying heavily on energy exports. Though
437 Algeria’s government has promoted agricultural development, yield is highly unstable due to
438 climate variability⁶⁷. This instability is likely to promote violence, particularly in agriculture
439 dependent areas as shown from our results (Fig. 3D). The contrasting indirect [negative] and
440 direct [positive] effects of temperature in Algeria are likely due to a positive temperature
441 effect on yield and a direct adverse influence of heat, which may be explained by the GAM.
442 In contrast, the influence of yield on violence risk was positive and significantly smaller in
443 Mali [50% smaller than in Algeria]. This is in spite of the fact that Mali’s economy is more
444 centered on agriculture than Algeria⁶⁸. Moreover, the positive yield effect was limited to the
445 northern part of Mali, which is less agricultural than its southern [and central] part (insert in
446 Fig. 3D).

447 Putting this in context, we know that most conflicts in Mali during the period of analysis
448 were intra-state conflicts between the government and the Tuareg nomadic inhabitants living
449 in the northern part of the country. Because our analysis is limited to small-scale conflicts,
450 the non-state, inter-group aspects of the Tuareg conflict, which occur primarily in the
451 northern, less agricultural part of the country, is well noted (Fig. 1A)⁶⁸. The Tuaregs are
452 primarily pastoral and as such continuously compete for scarce resources between pastoral
453 groups and with the few crop farmers and settled villagers in the north⁶⁸. Tuareg conflict is
454 believed to be an example of a resource conflict driven by climatic changes⁶⁹ and the
455 positive effect of yield on violence risk in our SEM is likely a reflection of this struggle, with
456 periods of increased yield in the northern region being a potential driver of ethnic tension and
457 inter-group violence.

458 These contrasting complex links in Algeria and Mali imply that the climate-violence
459 linkage should be investigated in the context of historical, geographical and ethnical
460 backgrounds of each location rather than as a general cross-sectional analysis. Such an
461 approach can shed light on contrasting effects of climate.

462 **6. Concluding Remarks**

463 Our findings reveal previously unreported effects of climate on risk of conflict outbreak.
464 More specifically, contrasting effects of temperature were detected at a regional scale and in
465 numerous countries in Africa and the ME. Importantly, temperature and rainfall direct effects
466 on conflict risk seem to be stronger than any indirect effect through resources such as water
467 availability and agricultural production (Fig. 3 and Table 1). This could mean one of three
468 things: that climate affects violence mostly through psychological and/or interactive
469 mechanisms [e.g. GAM and RAT^{17,18}]; that indirect effects depend on aspects of climate
470 variability that we have not considered⁷⁰; or that underlying mechanisms in which resource
471 scarcity or conflict-relevant abundance patterns affect violence are more complex than those
472 modeled by our SEMs.

473 As in previous studies²¹, the use of explicit controls affected the strength of the climate
474 effect in our SEMs [i.e. the difference between total and direct effects in Table 1], in our case
475 by up to 46%. This was important enough to expose indirect rain effects in Africa (Table 1).
476 It is important to note that the SEMs, although statistically significant (table S4), confirming
477 the validity of the a priori hypothesis, had very little predictive power [with 1st and 3rd
478 quantiles being 1.6% and 11% across countries] (table S5). This means that although our
479 SEMs did confirm impacts of climate on armed conflicts by effectively quantifying its direct
480 and indirect effects, these effects were relatively small compared to unobserved factors like
481 political, ethnic and likely other unaccounted socioeconomic factors. These were only partly

482 considered in our analysis, due to the difficulty to account for such factors at a grid-cell level,
483 in the form of next-year violence risk, which was shown to be greatly affected by present
484 year violence (explaining between 10% and 16% of the variance, at the continental level; Fig.
485 2B to D).

486 Our results demonstrate that no single proposed climate-conflict mechanism can alone
487 explain the empirical patterns that underlie the climate-conflict linkage across contrasting
488 regions or countries, and that this linkage is more complex than some analyses have
489 previously suggested²¹. We conclude that extreme caution should be exercised when
490 attempting to explain or project local climate-violence relationships on the basis of a single,
491 generalized theory. Large scale cross-sectional studies can be useful for identifying general
492 associations and trends, but an appropriately scaled and structured analysis is required to
493 explain and, potentially, address climate-violence risk factors in geographic context.

494 **Acknowledgment**

495 Authors thank C. Helman for helping to organize the data for the analyses, A. Mussery for
496 helping to organize the SEMs results in the SM, and two anonymous reviewers for insightful
497 comments. D.H. is a USA-Israel Fulbright Fellow for 2018/2019. C.F. is supported by the US
498 Geological Survey Drivers of Drought program and the US Agency for International
499 Development's Famine Early Warning Systems Network.

500 **References**

- 501 1. Scheffran, J., Brzoska, M., Kominek, J., Link, P. M. & Schilling, J. Climate change
502 and violent conflict. *Science* (80-). **336**, 869–871 (2012).
- 503 2. Hsiang, S. M., Meng, K. C. & Cane, M. A. Civil conflicts are associated with the
504 global climate. *Nature* **476**, 438–441 (2011).
- 505 3. Bernauer, T., Böhmelt, T. & Koubi, V. Environmental changes and violent conflict.
506 *Environ. Res. Lett.* **7**, 15601 (2012).
- 507 4. Koubi, V. Climate Change and Conflict. *Annu. Rev. Polit. Sci.* **22**, 343–360 (2019).
- 508 5. Koubi, V. Climate Change, the Economy, and Conflict. *Curr. Clim. Chang. Reports* **3**,
509 200–209 (2017).
- 510 6. Hodler, R. & Raschky, P. A. Economic shocks and civil conflict at the regional level.
511 *Econ. Lett.* **124**, 530–533 (2014).
- 512 7. Dube, O. & Vargas, J. F. Commodity Price Shocks and Civil Conflict: Evidence from
513 Colombia. *Rev. Econ. Stud.* **80**, 1384–1421 (2013).
- 514 8. Harris, G. & Vermaak, C. Economic inequality as a source of interpersonal violence:
515 Evidence from Sub-Saharan Africa and South Africa. *South African Journal of*
516 *Economic and Management Sciences* **18**, 45–57 (2015).
- 517 9. Zhang, D. D. *et al.* The causality analysis of climate change and large-scale human
518 crisis. *Proc. Natl. Acad. Sci.* **108**, 17296 LP – 17301 (2011).
- 519 10. Carleton, T. A. & Hsiang, S. M. Social and economic impacts of climate. *Science* (80).
520 **353**, (2016).
- 521 11. Fjelde, H. & von Uexkull, N. Climate triggers: rainfall anomalies, vulnerability and
522 communal conflict in sub-Saharan Africa. *Polit. Geogr.*, 31:444–453, (2012).
- 523 12. Wischnath, G. & Buhaug, H. Rice or riots: On food production and conflict severity

- 524 across India. *Polit. Geogr.*, 43, 6-15, (2014).
- 525 13. Salehyan, I. & Hendrix C. S. Climate shocks and political violence. *Glob Environ*
526 *Change* 28:239–250, (2014).
- 527 14. Witsenburg, K. M. & Adano, W. R. Of rain and raids: violent livestock raiding in
528 Northern Kenya. *Civil Wars* 11:514–538, (2009).
- 529 15. Raleigh, C. & Kniveton, D. Come rain or shine: An analysis of conflict and climate
530 variability in East Africa. *J. Peace Res.*, 49(1), 51-64, (2012).
- 531 16. Nordkvelle, J., Rustad, S. A. & Salmivalli, M. Identifying the effect of climate
532 variability on communal conflict through randomization. *Clim. Change*, 141(4), 627-
533 639, (2017).
- 534 17. Dewall, C. N., Anderson, C. A. & Bushman, B. J. The general aggression model:
535 Theoretical extensions to violence. *Psychol. Violence* 1, 245–258 (2011).
- 536 18. Cohen, L. E. & Felson, M. Social change and crime rate trends : A Routine Activity
537 Approach. *Am. Sociol. Rev.* 44, 588–608 (1979).
- 538 19. O’Loughlin, J., Linke, A. M. & Witmer, F. D. W. Effects of temperature and
539 precipitation variability on the risk of violence in sub-Saharan Africa, 1980-2012.
540 *Proc. Natl. Acad. Sci. U. S. A.* 111, 16712–16717 (2014).
- 541 20. O’Loughlin, J. *et al.* Climate variability and conflict risk in East Africa, 1990–2009.
542 *Proc. Natl. Acad. Sci.* 109, 18344–18349 (2012).
- 543 21. Hsiang, S. M., Burke, M. & Miguel, E. Quantifying the influence of climate on human
544 conflict. *Science (80-)*. 341, (2013).
- 545 22. Hsiang, S. M. & Burke, M. Climate, conflict, and social stability: what does the
546 evidence say? *Clim. Change* 123, 39–55 (2014).
- 547 23. Helman, D. & Zaitchik, B. F. Temperature anomalies affect violent conflicts in
548 African and Middle Eastern warm regions. *Glob Environ Chang.* (2020).
- 549 24. Ide, T. Research methods for exploring the links between climate change and conflict.
550 *Wiley Interdiscip. Rev. Clim. Chang.* 8, (2017).
- 551 25. Buhaug, H. Climate not to blame for African civil wars. *Proc. Natl. Acad. Sci. U. S. A.*
552 107, 16477–16482 (2010).
- 553 26. Adams, C., Ide, T., Barnett, J. & Detges, A. Sampling bias in climate-conflict research.
554 *Nat. Clim. Chang.* 8, 200–203 (2018).
- 555 27. Buhaug, H. *et al.* One effect to rule them all? A comment on climate and conflict.
556 *Clim. Change* 127, 391–397 (2014).
- 557 28. Mach, K. J. *et al.* Climate as a risk factor for armed conflict. *Nature* 571, 193–197
558 (2019).
- 559 29. Sundberg, R. & Melander, E. Introducing the UCDP georeferenced event dataset. *J.*
560 *Peace Res.* 50, 523–532 (2013).
- 561 30. Chou, C.-P. & Bentler, P. M. Estimates and tests in structural equation modeling. in
562 *Structural equation modeling: Concepts, issues, and applications.* 37–55 (Sage
563 Publications, Inc, 1995).
- 564 31. Sundberg, R. & Croicu, M. UCDP Non-State Conflict Codebook Version 18.1.
565 *Uppsala Confl. Data Progr. Web Page* 1–10 (2017).

- 566 32. Carpenter, T. G. Tangled web: The Syrian civil war and its implications. *Mediterr. Q.*
567 **24**, 1–11 (2013).
- 568 33. Funk, C. *et al.* A high-resolution 1983–2016 Tmax climate data record based on
569 infrared temperatures and stations by the climate hazard center. *J. Clim.* **32**, 5639–
570 5658 (2019).
- 571 34. Funk, C. *et al.* The climate hazards infrared precipitation with stations—a new
572 environmental record for monitoring extremes. *Sci. Data* **2**, 150066 (2015).
- 573 35. Dinku, T. *et al.* Validation of the CHIRPS satellite rainfall estimates over eastern
574 Africa. *Q. J. R. Meteorol. Soc.* **144**, 292–312 (2018).
- 575 36. Maidment, R. I., Allan, R. P. & Black, E. Recent observed and simulated changes in
576 precipitation over Africa. *Geophys. Res. Lett.* **42**, 8155–8164 (2015).
- 577 37. Center for International Earth Science Information Network. - CIESIN - Columbia
578 University. 1999. Poverty Mapping Project: Global Subnational Infant Mortality
579 Rates. Palisades, NY: NASA Socioeconomic Data and Applications Center (SEDAC)
580 [Accessed: 17 February 2019]. Available at: <https://doi.org/10.7927/H4PZ56R2>.
- 581 38. Von Uexkull, N., Croicu, M., Fjelde, H. & Buhaug, H. Civil conflict sensitivity to
582 growing-season drought. *Proc. Natl. Acad. Sci. U. S. A.* **113**, 12391–12396 (2016).
- 583 39. ESA: *Land Cover CCI Product User Guide Version 2.0* [Last access: 17 June 2019].
584 (2019).
- 585 40. Liu, X. *et al.* Comparison of country-level cropland areas between ESA-CCI land
586 cover maps and FAOSTAT data. *Int. J. Remote Sens.* **39**, 6631–6645 (2018).
- 587 41. Didan, K. *et al.* *Multi-Sensor Vegetation Index and Phenology Earth Science Data*
588 *Records Algorithm Theoretical Basis Document And User Guide Version 4.0.* (2015).
- 589 42. Jiang, Z., Huete, A. R., Didan, K. & Miura, T. Development of a two-band enhanced
590 vegetation index without a blue band. *Remote Sens. Environ.* **112**, 3833–3845 (2008).
- 591 43. Huete, A. *et al.* Overview of the radiometric and biophysical performance of the
592 MODIS vegetation indices. *Remote Sens. Environ.* **83**, 195–213 (2002).
- 593 44. Huang, X., Xiao, J. & Ma, M. Evaluating the Performance of Satellite-Derived
594 Vegetation Indices for Estimating Gross Primary Productivity Using FLUXNET
595 Observations across the Globe. *Remote Sensing* **11**, (2019).
- 596 45. Helman, D., Mussery, A., Lensky, I. M. & Leu, S. Detecting changes in biomass
597 productivity in a different land management regimes in drylands using satellite-derived
598 vegetation index. *Soil Use Manag.* **30**, (2014).
- 599 46. Helman, D., Lensky, I. M., Mussery, A. & Leu, S. Rehabilitating degraded drylands by
600 creating woodland islets: Assessing long-term effects on aboveground productivity and
601 soil fertility. *Agric. For. Meteorol.* **195–196**, (2014).
- 602 47. Helman, D. Land surface phenology: What do we really ‘see’ from space? *Sci. Total*
603 *Environ.* **618**, 665–673 (2018).
- 604 48. Gitelson, A. A. *et al.* Relationship between gross primary production and chlorophyll
605 content in crops: Implications for the synoptic monitoring of vegetation productivity.
606 *J. Geophys. Res. Atmos.* **111**, (2006).
- 607 49. FAO. Production Database. Crops Dataset. Latest update: November 2016 [Accessed:
608 18 June 2019].

- 609 50. NOAA. Defense Meteorological Satellite Program (DMSP)—Data Archive, Research,
610 and Products [Internet] Earth Observation Group, Boulder [cited 2020]. Available at:
611 <http://ngdc.noaa.gov/eog/dmsp.html>.
- 612 51. Levin, N., Ali, S. & Crandall, D. Utilizing remote sensing and big data to quantify
613 conflict intensity: The Arab Spring as a case study. *Appl. Geogr.* **94**, 1–17 (2018).
- 614 52. Ivan, K., Holobăcă, I.-H., Benedek, J. & Török, I. Potential of Night-Time Lights to
615 Measure Regional Inequality. *Remote Sensing* **12**, (2020).
- 616 53. Bagan, H., Borjigin, H. & Yamagata, Y. Assessing nighttime lights for mapping the
617 urban areas of 50 cities across the globe. *Environ. Plan. B Urban Anal. City Sci.* **46**,
618 1097–1114 (2018).
- 619 54. Li, S., Zhang, T., Yang, Z., Li, X. & Xu, H. Night Time Light Satellite Data for
620 Evaluating the Socioeconomics in Central Asia. *ISPRS - Int. Arch. Photogramm.*
621 *Remote Sens. Spat. Inf. Sci.* **42W7**, 1237–1243 (2017).
- 622 55. Proville, J., Zavala-Araiza, D. & Wagner, G. Night-time lights: A global, long term
623 look at links to socio-economic trends. *PLoS One* **12**, 1–12 (2017).
- 624 56. Stevens, F. R., Gaughan, A. E., Linard, C. & Tatem, A. J. Disaggregating census data
625 for population mapping using Random forests with remotely-sensed and ancillary data.
626 *PLoS One* **10**, 1–22 (2015).
- 627 57. Kumar, S. V *et al.* Land information system: An interoperable framework for high
628 resolution land surface modeling. *Environ. Model. Softw.* **21**, 1402–1415 (2006).
- 629 58. Niu, G.-Y. *et al.* The community Noah land surface model with multiparameterization
630 options (Noah-MP): 1. Model description and evaluation with local-scale
631 measurements. *J. Geophys. Res. Atmos.* **116**, (2011).
- 632 59. Getirana, A. C. V *et al.* The Hydrological Modeling and Analysis Platform (HyMAP):
633 Evaluation in the Amazon Basin. *J. Hydrometeorol.* **13**, 1641–1665 (2012).
- 634 60. Gelaro, R. *et al.* The Modern-Era Retrospective Analysis for Research and
635 Applications, Version 2 (MERRA-2). *J. Clim.* **30**, 5419–5454 (2017).
- 636 61. Hegre, H. & Sambanis, N. Sensitivity analysis of empirical results on civil war onset.
637 *J. Conflict Resolut.* **50**, 508–535 (2006).
- 638 62. Baron, R. A. & Ransberger, V. M. Ambient temperature and the occurrence of
639 collective violence: The ‘long, hot summer’ revisited. *Journal of Personality and*
640 *Social Psychology* **36**, 351–360 (1978).
- 641 63. Bell, P. A. & Baron, R. A. Aggression and Heat: The Mediating Role of Negative
642 Affect1. *J. Appl. Soc. Psychol.* **6**, 18–30 (1976).
- 643 64. Baron, R. A. Aggression as a function of ambient temperature and prior anger arousal.
644 *Journal of Personality and Social Psychology* **21**, 183–189 (1972).
- 645 65. Baron, R. A. & Bell, P. A. Aggression and heat: The influence of ambient temperature,
646 negative affect, and a cooling drink on physical aggression. *J. Pers. Soc. Psychol.* **33**,
647 245–255 (1976).
- 648 66. Anderson, C. A. Temperature and Aggression: Ubiquitous Effects of Heat on
649 Occurrence of Human Violence. *Psychol. Bull.* **106**, 74–96 (1989).
- 650 67. Amine, B. M. & Fatima, B. Determinants of on-farm diversification among rural
651 households: Empirical evidence from Northern Algeria. *International Journal of Food*

- 652 *and Agricultural Economics (IJFAEC)* **04**, 87–99
- 653 68. Keita, K. Conflict and conflict resolution in the Sahel: The Tuareg insurgency in Mali.
654 *Small Wars Insur.* **9**, 102–128 (1998).
- 655 69. Bächler, G. *Violence through environmental discrimination: Causes, Rwanda arena,*
656 *and conflict model.* **2**, (Kluwer Academic, 1998).
- 657 70 Buhaug, H. Climate–conflict research: some reflections on the way forward. *Wiley*
658 *Interdisciplinary Reviews: Climate Change*, 6(3), 269-275 (2015).